# Study of Nuclear Stopping in Central Collisions at Intermediate Energies

G. Lehaut,[1,2] D. Durand,[1] O. Lopez,[1] E. Vient,[1] A. Chbihi,[3] J. D. Frankland,[3] E. Bonnet,[3] B. Borderie,[4] R. Bougault,[1] E. Galichet,[4,5] D. Guinet,[2] Ph. Lautesse,[2] N. Le Neindre,[1] P. Napolitani,[4] M. Parlog,[1] M. F. Rivet,[4] and E. Rosato[6]

(INDRA and ALADIN Collaborations)

[1]*LPC, CNRS/IN2P3, Ensicaen, Université de Caen Basse Normandie, F-14050 Caen cedex, France*
[2]*Université de Lyon, Université Lyon 1, CNRS-IN2P3, Institut de Physique Nucléaire de Lyon, F-69622 Villeurbanne, France*
[3]*GANIL, DSM-CEA/CNRS/IN2P3, F-14076 Caen cedex, France*
[4]*Institut de Physique Nucléaire, IN2P3-CNRS and Université Paris-Sud, 91405 Orsay cedex, France*
[5]*Conservatoire National des Arts et Métiers, F-75141 Paris, France*
[6]*Dipartimento di Scienze Fisiche e Sezione INFN, Université di Napoli "Federico II," I-80126 Napoli, Italy*
(Received 10 February 2010; published 9 June 2010)

Nuclear stopping has been investigated in central nuclear collisions at intermediate energies by analyzing kinematically complete events recorded with the help of the $4\pi$ multidetector INDRA for a large variety of symmetric systems. It is found that the mean isotropy ratio defined as the ratio of transverse to parallel momenta (energies) reaches a minimum near the Fermi energy, saturates or slowly increases depending on the mass of the system as the beam energy increases, and then stays lower than unity, showing that significant stopping is not achieved even for the heavier systems. Close to and above the Fermi energy, experimental data show no effect of the isospin content of the interacting system. A comparison with transport model calculations reveals that the latter overestimates the stopping power at low energies.

DOI: 10.1103/PhysRevLett.104.232701 PACS numbers: 25.70.−z, 21.65.Mn

The study of transport phenomena in nuclear reactions at intermediate energies is of major importance in the understanding of the fundamental properties of nuclear matter (for an introduction, see [1]). On the one hand, the transport properties are critical to describe the process of supernova collapse and the formation of a neutron star [2]. On the other hand, nuclear stopping governs the amount of dissipated energy, the amplitude of large collective motion, and the competition between various mechanisms such as deep inelastic reactions, neck emission, and fusion reactions [3]. The comparison of the predictions of the microscopic transport models (see, for instance, [4–11]) with experimental data can help to improve our knowledge of the basic ingredients of such models: namely, the nuclear equation of state and, as such, the in-medium properties of the nucleon-nucleon interaction. In this context, it is mandatory to test the different models over a broad systematics in system size and incident energy.

For the system Au + Au in the energy range 90*A*–1930*A* MeV, the FOPI Collaboration observed a plateau of maximal stopping in the interval 200*A*–800*A* MeV [10]. In this paper we will explore the low energy range, below and above the Fermi energy (10*A*–100*A* MeV), where the transition between mean field and nucleon-nucleon collision effects occurs. This is achieved by analyzing high quality data collected for a large variety of systems with the INDRA multidetector at GANIL (see, for instance, [12–16]) and at GSI [17,18]. Symmetric systems with total sizes between 80 and 400 mass units and at incident energies between 12*A* and 100*A* MeV have been considered. Taking into account the experimental detection thresholds in the backward part of the detection device, only charged products which are emitted in the forward velocity space in the center of mass of the reaction are analyzed. Thus, the effects of the thresholds are minimized as are the associated distortions on the global variables considered in the following. The selection criterion, as far as the quality of the data is concerned, was the following: events were retained if the total detected charge $Z_{\mathrm{tot}}$ (neutrons were not detected) in the forward hemisphere of the center of mass was larger than 80% of the projectile charge (corresponding to half of the total charge of the system). Contrary to the study of the FOPI data presented in [19], no attempt has been made to symmetrize the data. In the following, we limit ourselves to the study of central collisions. Event selection based on minimum bias effects is needed to avoid autocorrelations. Since quantities involving both the transverse and longitudinal directions are considered in the following, it is not suitable to use vector variables such as, for instance, the transverse energy [14,20]. Thus, a scalar variable is desirable, and a natural choice is the total multiplicity of detected charged products, $N_{\mathrm{ch}}$. In order to quantify the stopping power, the usual observable is the ratio of transverse to parallel quantities like the energy-based isotropy ratio $R_E$, defined as

 

$$R_E = \frac{\sum E_\perp}{2\sum E_\parallel}, \quad (1)$$

where $E_\perp$ ($E_\parallel$) is the c.m. transverse (parallel) energy and the sum runs over all products with the above-mentioned selection. In the following, we will also use $R_p$, defined as

$$R_p = \frac{2\sum p_\perp}{\pi\sum p_\parallel}, \quad (2)$$

where momenta ($mv$) are used instead of energies; since INDRA does not detect masses for $Z > 4$, heavier fragment masses are estimated from a parametrization of the $\beta$-stability valley.

We now discuss how the value of the isotropy ratio for central collisions, $R_E^{\rm central}$, is obtained. Figure 1(a) shows the distribution of the total multiplicity, $N_{\rm ch}$, for the Xe + Sn system at 50$A$ MeV. It exhibits the usual shape, with a first contribution at low values corresponding to peripheral collisions followed by a bump associated with more dissipative (central and midcentral) reactions. The total measured cross section is 3.4 b for $N_{\rm ch} \geq 4$, to be compared to the calculated reaction cross section of 6 b [21], and the mean percentage of events fulfilling the condition on the total detected charge is about 40%. The filled area is then associated with central collisions and corresponds to a cross section of 50 mb. This is the typical cross section for all systems considered in this work. The cut in multiplicity is based on the results of Figs. 1(b) and 1(d) in which the mean value $\langle R_E \rangle$ is superimposed over the bi-dimensional plot $R_E$-$N_{\rm ch}$. It is worth noting from Fig. 1(b) that the largest fluctuations of $R_E$ are not associated with the largest values of the multiplicity. This could suggest that the selection of central events by means of $N_{\rm ch}$ is inappropriate. However, an important effect to consider is the influence of the statistics of the multiplicity distribution: this has been accounted for in Fig. 1(d) by dividing the contents of each bin by the number of events with the corresponding multiplicity obtained from Fig. 1(a). Figure 1(d) shows that the shape of the $R_E$ distribution has no further significant evolution above $N_{\rm ch} = 36$. Choosing this multiplicity as a cut is thus a compromise between a sizable cross section compatible with central collisions and a stabilization of the isotropy ratio. The resulting distribution of $R_E$ for central collisions is shown in Fig. 1(c), from which the mean values $R_E^{\rm central}$ and the corresponding widths $\sigma_{R_E^{\rm central}}$ are obtained. The statistical error on the value of $R_E^{\rm central}$ is obtained following $\delta R_E^{\rm central} = \frac{\sigma_{R_E^{\rm central}}}{\sqrt{N_{\rm evt}}}$, where $N_{\rm evt}$ is the number of selected events. Typically, $\sigma_{R_E^{\rm central}}$ is around 0.5 and $N_{\rm evt}$ is of the order of several tens of thousands [see Fig. 1(c)]. Thus, the statistical error is typically a fraction of a percent.

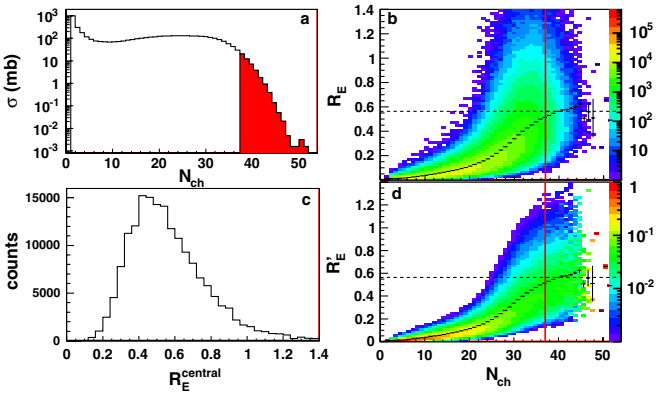


FIG. 1 (color online). Data for $^{129}$Xe + $^{119}$Sn collisions at 50$A$ MeV. (a) Distribution of total charged particle multiplicity $N_{\rm ch}$. The dark area corresponds to central events retained for the analysis of the stopping power. (b) Bi-dimensional plot showing the correlation between the isotropy ratio and the total multiplicity. (c) Distribution of $R_E$ for central collisions. (d) Same as (b), but after renormalizing the number of events in each multiplicity bin.

Systematic errors have been estimated by varying the multiplicity cut for light systems (Ar + KCl, Ni + Ni) by 1 unit and by 2 to 3 units for heavy systems (Xe + Sn, Au + Au) in order to change all cross sections in the same proportion. These errors are reported in Fig. 2. Note that hot nuclei or sources from quasifusion, which are used to search and study a phase transition of the liquid-gas type, are not selected with the total charged product multiplicity. Sources associated with a larger stopping can be selected using topology selectors (see [22] for details), and due to fluctuations (see Fig. 1), they cover a rather broad range in total charged product multiplicity [23].

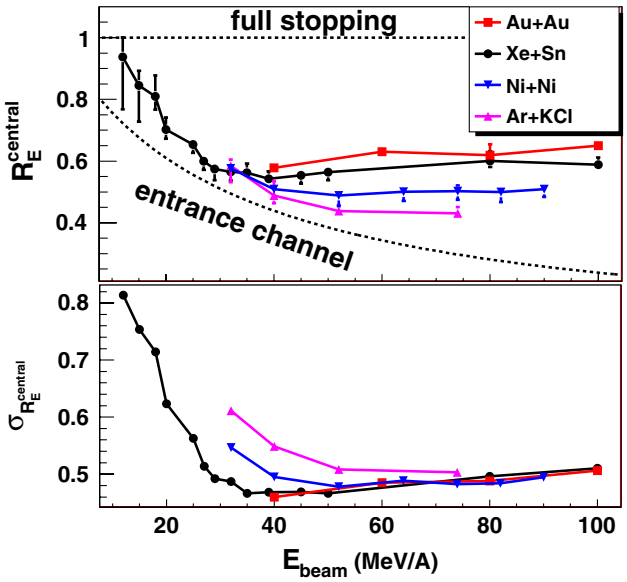


FIG. 2 (color online). Top panel: evolution of $R_E^{\rm central}$ as a function of beam energy. Data are for central collisions and for four different systems indicated in the inset; error bars are systematics, and the dashed line $R_{\rm iso}^{\rm central}$ is from the initial momentum distribution (see text). Bottom panel: evolution of $\sigma_{R_E^{\rm central}}$ versus beam energy.

The present method has been used for a large bunch of experimental data covering the intermediate energy range from 10*A*–100*A* MeV and for systems from about 80 (Ar + KCl) up to nearly 400 mass units (Au + Au). Results are displayed in Fig. 2 which shows the evolution of $R_E^{\mathrm{central}}$ and $\sigma_{R_E^{\mathrm{central}}}$ as a function of the beam energy. The upper panel of the figure shows a decrease of $R_E^{\mathrm{central}}$ from 10*A* to 40*A* MeV (only the Xe + Sn system is available in this energy range). The strong decrease of the fusion cross section of light systems in this bombarding energy range supports the fact that the stopping power decreases [24]. For beam energies above the Fermi energy, the isotropy ratio reaches a plateau, the value of which increases with the mass of the system. The larger the mass, the larger $R_E^{\mathrm{central}}$ is. In any case, low values far from unity are observed. However, it should be realized that such a value cannot be reached even for $b = 0$ collisions due to geometrical (corona) effects [25]. The widths (Fig. 2, bottom panel) follow the same trends as the isotropy ratio. Around 30*A* MeV, lighter systems show larger fluctuations than heavy ones due to particle number effects. As energy increases the width values for all systems tend to merge, suggesting that, when the multiplicity cut reaches a high enough value (of the order of 15), the increase of the width is related to intrinsic fluctuations, whatever the number of particles. It may be noted that the beam energy where the merging occurs has the same dependence on the system mass as the transition energy from the order to disorder regime seen in the universal fluctuations of the largest fragment [26].

The dashed line in Fig. 2 (top panel, labeled ''entrance channel'') is the value of the isotropy ratio $R_E$ calculated for a momentum distribution of two sharp Fermi spheres (no temperature) separated by the relative velocity between the projectile and the target in the entrance channel (no dissipation). Thus, the distance between the experimental points and the dashed line is a ''measure'' of the influence of the one-body and two-body dissipations on the isotropy ratio. The general evolution of the data is interpreted as a transition from the dominant influence of the mean field at low energy (one-body dissipation which does not depend on the size of the system) towards the dominance of in-medium nucleon-nucleon collisions at higher energy (two-body dissipation depending on the size of the system). As beam energy increases up to the Fermi energy, the nuclear mean field is less and less efficient in stopping the two incoming nuclei. This is accompanied by an increase of preequilibrium emission leading to a decrease of the isotropy ratio. Close to the Fermi energy, all studied systems have more or less the same isotropy ratio (between 0.5 and 0.6) with a value close to the entrance channel limit. It is worth noting that this incident energy also corresponds to the onset of radial flow as reported in [22]. Above the Fermi energy, phase space opens up gradually for in-medium two-body collisions since more and more final states are accessible during the nucleon-nucleon diffusion. Larger momentum transfers are possible. Collisions are then essentially governed by the nucleon mean free path and the size of the system: the larger the system, the larger the number of nucleon-nucleon collisions is and, as such, the larger the stopping power is. This is confirmed by the data, the stopping being maximum for the Au + Au system, while for the lighter system (Ar + KCl), the isotropy ratio still decreases and hardly stabilizes around 60*A* MeV. Note that even for heavy systems, the increase is very moderate, agreeing with the fact that the nucleon mean free path remains large (no full stopping) throughout the intermediate energy range.

We will now compare our data with a microscopic transport model. In [27], extensive calculations concerning Sn + Sn central collisions in the Fermi energy range are reported. This system is close to the INDRA Xe + Sn system so that a comparison is made possible using the isotropy ratio based on momenta defined by Eq. (2). Isospin-dependent quantum molecular dynamics (IQMD) have been used with a modified version of nucleon-nucleon cross-section terms, an isoscalar nuclear potential with $K_\infty = 216$ MeV, and different isovector potentials [2]. One of the main conclusions of the study was that the symmetry potential $U_1^{\mathrm{sym}}$ ( $\propto \rho/\rho_0$) does not play an important role as far as the stopping power is concerned. At variance, the latter is rather sensitive to the isospin dependence of the in-medium nucleon-nucleon cross section $\sigma_{\mathrm{nn}}$. The same findings have also been reported in [11]. Following these conclusions, in Fig. 3 we superimpose on our data the IQMD results for a fixed symmetry potential $U_1^{\mathrm{sym}}$ and two different versions of the in-medium nucleon-nucleon cross-section term. The first one considers the different experimental neutron-proton, neutron-neutron, and proton-proton cross sections and is called the

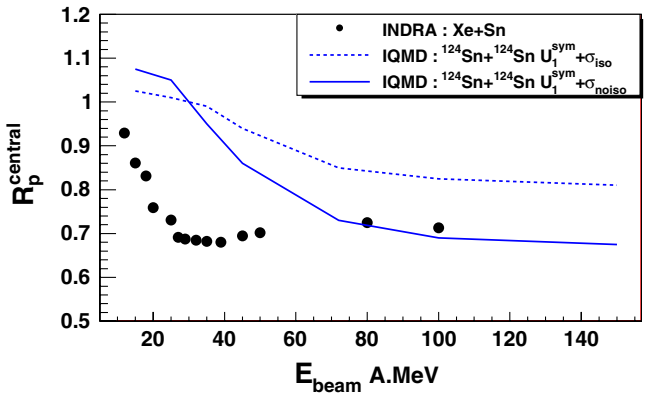


FIG. 3 (color online). Comparison between experimental $R_p^{\mathrm{central}}$ values (black points) and predictions of IQMD calculations [27] (lines) for central Xe + Sn collisions (Sn + Sn in the IQMD case). The dashed line is for isospin-dependent in-medium nucleon-nucleon collisions, while the solid line is for no isospin dependence. Note here that $R_p^{\mathrm{central}}$ is used instead of $R_E^{\mathrm{central}}$ as in Fig. 1.

TABLE I. Values of $R_E^{\text{central}}$ for different Xe + Sn systems at 32$A$, 45$A$, and 100$A$ MeV.

| System | $N/Z$ | 32 MeV/$A$ | 45 MeV/$A$ | 100 MeV/$A$ |
|---|---|---|---|---|
| $^{124}$Xe + $^{112}$Sn | 1.27 | 0.54 | 0.53 | 0.58 |
| $^{129}$Xe + $^{112}$Sn | 1.32 | ··· | ··· | 0.60 |
| $^{124}$Xe + $^{124}$Sn | 1.38 | 0.54 | ··· | 0.56 |
| $^{129}$Xe + $^{nat}$Sn | 1.38 | 0.55 | 0.53 | ··· |
| $^{136}$Xe + $^{112}$Sn | 1.38 | 0.50 | 0.54 | ··· |
| $^{129}$Xe + $^{124}$Sn | 1.43 | ··· | ··· | 0.59 |
| $^{136}$Xe + $^{124}$Sn | 1.5 | 0.49 | 0.52 | ··· |

isospin-dependent cross section $\sigma_{\text{iso}}$. The second one, $\sigma_{\text{noiso}}$, considers the same cross section for all the isospin channels and is taken as the experimental neutron-neutron cross section [28]. The calculations agree with our data at incident energies above 60$A$ MeV and for the collision term without isospin dependence ($\sigma_{\text{noiso}}$). At lower incident energies, the model overestimates the experimental data by giving too much stopping.

We now come to the last part of the study, namely, the influence of the isospin content of the system on the value of the stopping power. Data are available for five (four) different Xe + Sn reactions at 32$A$ (45$A$ and 100$A$) MeV. Central collisions have been selected as before and the resulting cross sections are comparable for all systems. Table I summarizes the results. Systematic errors are not reported here but are similar to the previous ones.

For a given beam energy, isotropy ratios are equal within the error bars, and one can reasonably conclude that the role of the isospin degree of freedom is negligible, as far as the stopping power is concerned, for all considered energies. At low energies, the effect of two-body dissipation is weak. On the other hand, IQMD calculations suggest that the form of the symmetry potential, and hence the isospin content of the system, has no major influence around 40$A$ MeV. Our data confirmed this trend. This result provides a strong constraint for transport theory and shows that the nuclear potential and the collision term have to be defined in a coherent way.

To conclude, the behavior of the isotropy ratio in central symmetric nuclear reactions at intermediate energies has been studied. It shows a rapid decrease as a function of the incident energy up to 40$A$ MeV(Fermi energy). For larger energies, the behavior depends on the mass of the system, showing the increasing role played by two-body dissipation. However, low values far from unity have been measured, indicating that significant stopping is not achieved in this energy regime even for the most central collisions and for the most massive systems. A comparison with IQMD calculation reveals that such a model overpredicts the stopping at low energies. At higher energies, results are in better agreement with a nonisospin-dependent collision term. Lastly, around 40$A$ and 100$A$ MeV, the role of the isospin content of the system is negligible as far as the stopping power is concerned. These findings show that the stopping power brings important information about the properties of the nuclear matter and call for more systematic comparisons with dynamical models.


[1] D. Durand, B. Tamain, and E. Suraud, *Nuclear Dynamics in the Nucleonic Regime* (Institute of Physics, New York, 2001).
[2] J. M. Lattimer and M. Prakash, Astrophys. J. **550**, 426 (2001).
[3] Eur. Phys. J. A **30** (2006), and reference therein.
[4] A. Ohnishi and J. Randrup, Phys. Rev. Lett. **75**, 596 (1995).
[5] J. Aichelin, Phys. Rep. **202**, 233 (1991).
[6] A. Bonasera *et al.*, Phys. Rep. **243**, 1 (1994).
[7] Ph. Chomaz *et al.*, Phys. Rev. Lett. **73**, 3512 (1994).
[8] A. Ono *et al.*, Phys. Rev. Lett. **68**, 2898 (1992).
[9] T. Gaitanos *et al.*, Phys. Lett. B **609**, 241 (2005).
[10] A. Andronic *et al.*, Eur. Phys. J. A **30**, 31 (2006).
[11] S. Kumar, S. Kumar, and R. K. Puri, Phys. Rev. C **81**, 014601 (2010).
[12] B. Borderie, J. Phys. G **28**, R217 (2002).
[13] N. Marie *et al.* (INDRA Collaboration), Phys. Lett. B **391**, 15 (1997).
[14] E. Plagnol *et al.* (INDRA Collaboration), Phys. Rev. C **61**, 014606 (1999).
[15] V. Métivier *et al.* (INDRA Collaboration), Nucl. Phys. **A672**, 357 (2000).
[16] S. Hudan, A. Chbihi, and J. D. Frankland *et al.* (INDRA Collaboration), Phys. Rev. C **67**, 064613 (2003).
[17] J. Łukasik *et al.* (INDRA and ALADIN Collaborations), Phys. Rev. C **66**, 064606 (2002).
[18] A. Le Fèvre *et al.* (INDRA and ALADIN Collaborations), Nucl. Phys. **A735**, 219 (2004).
[19] W. Reisdorf *et al.* (FOPI Collaboration), Phys. Rev. Lett. **92**, 232301 (2004).
[20] J. Łukasik *et al.* (INDRA Collaboration), Phys. Rev. C **55**, 1906 (1997).
[21] S. Kox, *et al.*, Nucl. Phys. **A420**, 162 (1984).
[22] B. Borderie and M. F. Rivet, Prog. Part. Nucl. Phys. **61**, 551 (2008).
[23] J. D. Frankland *et al.*, Nucl. Phys. **A689** 905 (2001).
[24] P. Lautesse *et al.*, Eur. Phys. J. A **27**, 349 (2006).
[25] W. Reisdorf *et al.*, Nucl. Phys. **A612**, 493 (1997).
[26] J. D. Frankland *et al.*, Phys. Rev. C **71**, 034607 (2005).
[27] J.-Y. Liu *et al.*, Phys. Rev. Lett. **86**, 975 (2001).
[28] J.-Y. Liu *et al.*, Phys. Rev. C **63**, 054612 (2001).